Cross-stream diffusion in bedload transport

Grégoire Seizilles, Eric Lajeunesse, Olivier Devauchelle, Michael Bak

Cross-stream diffusion in bedload transport

Grégoire Seizilles,[1] Eric Lajeunesse,[1] Olivier Devauchelle,[1] and Michael Bak[2]

[1] *Institut de Physique du Globe - Sorbonne Paris Cité, Équipe de Dynamique des fluides géologiques, 1 rue Jussieu, 75238 Paris cedex 05, France.*

[2] *Department of Earth and Environmental Science, University of Pennsylvania, 154A Hayden Hall/6316, 240 S. 33rd St., Philadelphia, PA 19104*

We investigate experimentally the statistical properties of bedload transport induced by a steady, uniform and laminar flow. We focus chiefly on lateral transport. The analysis is restricted to experiments where the flow-induced shear stress is just above the threshold for sediment transport. We find that, in this regime, the concentration of moving particles is low enough to neglect interactions between themselves. We can therefore represent bedload as a thin layer of independent walkers travelling over the bed surface. In addition to their downstream motion, the particles show significant fluctuations of their cross-stream velocity, likely due to the roughness of the underlying sediment bed. This causes particles to disperse laterally. Based on thousands of individual trajectories, we show that this lateral spreading is the manifestation of a random walk. The experiments are entirely consistent with Fickian diffusion.

I. INTRODUCTION

When a fluid runs over a granular bed, it applies a shear stress on the superficial layer of grains. If the stress exceeds a threshold, some grains are entrained by the flow. Their displacement then deforms the bed, and the resulting interaction between flow and sediment transport generates a beautiful variety of river shapes and coastal morphologies[1–4]. Understanding this process requires a sound theory of bedload transport.

At moderate shear stress, the particles move by a combination of rolling, sliding, and bouncing, while gravity maintains them close to the bed surface. The layer of entrained grains, referred to as "bedload layer", is only a few grain-diameters thick. Due to this confinement, and contrary to transport in suspension, shear stress is the primary control on bedload transport. As it increases, bedload transport intensifies[5–14].

Laboratory observations reveal that the bedload layer continuously exchanges particles with the sediment bed[9,12,13,15,16]. According to the "erosion-deposition model", initially established for viscous flows[15,17] and later extended to turbulent flows[16], the equilibration of this exchange sets the surface concentration n of the bedload layer (n is the number of moving particles per unit bed area). This theory proved versatile enough to describe the formation of various bedforms[17–19] and the transport of mixed grain sizes[20].

The erosion-deposition model treats the bedload layer as a uniform reservoir of independent particles. Accordingly, the bedload flux q_x simply reads

$$q_x = V_x\, n\,, \tag{1}$$

where V_x is the average particle velocity. This statistical interpretation proves reasonable over a broad range of shear stress[15,16,21]. At high shear stress, however, the bedload layer becomes denser and moving particles interact with each other. The momentum exchange between grains then plays a significant role[22,23], and the erosion-deposition model breaks down.

A series of recent papers provide insight on higher-order moments of the velocity distribution, paving the way for a thorough statistical theory of bedload transport[24–26]. In particular, the dispersion of the streamwise particle velocity around the mean V_x generates longitudinal dispersion[27]. In addition, several authors have observed that, as bedload particles move downstream, their cross-stream velocity fluctuates around zero, with a symmetric exponential distribution[15,16,25]. By itself, this observation suggests that the convective motion embodied in equation (1) is accompanied by particle diffusion. To our knowledge, the diffusion of bedload particles across the flow direction has never been investigated. The present paper aims at quantifying this phenomenon, by tracking the trajectories of bedload particles in a laminar laboratory channel.
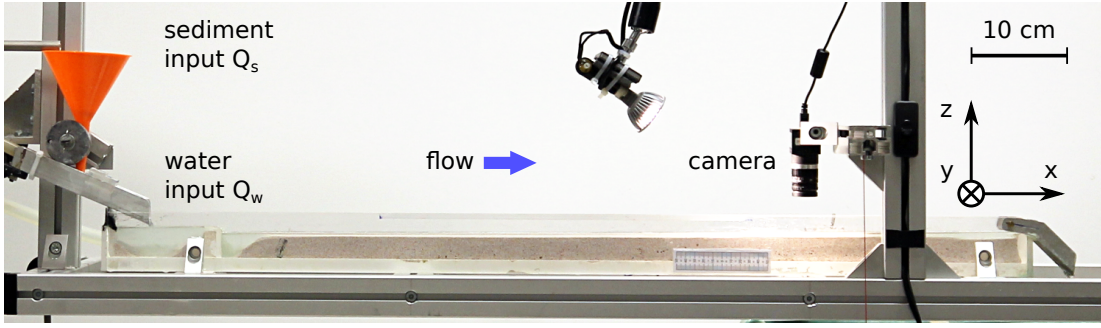
FIG. 1. Experimental laminar channel. Water and sediments are introduced at constant rate from the left end. The video camera records the trajectories of bedload particles through the water surface. The channel is 1 m-long and its width is $W = 3$ cm. Its slope in the x-direction is about $S \sim 0.007 - 0.016$.

When interactions between moving particles are negligible, the macroscopic transport is simply the superposition of independent trajectories, making its statistical analysis straightforward. We expect this assumption to hold in the low concentration limit ($n\,d_s^2 \ll 1$, where d_s is the grain size), that is, when the shear stress hardly suffices to transport a few particles. Fortunately, a low concentration also simplifies particle tracking. Therefore, the experiments and the theory presented here are restricted to near-threshold conditions. We believe this is typical of many natural systems, since alluvial rivers often maintain their bed just above the threshold of motion[28–30].

II. TRANSPORT NEAR THRESHOLD

A. Experimental set-up

A straight channel (length 1 m, width $W = 3$ cm, figure 1) is filled with plastic sediments (density $\rho_s = 1520 \pm 50$ g/L, diameter $d_s = 344 \pm 90$ μm). The grains are irregularly shaped, with sharp angles (Guyblast type II, grade 30–40, Guyson).

As water flows above the 3 cm-thick granular layer, superficial grains are entrained towards the outlet, while their trajectory is recorded with a video camera. We introduce water and grains at constant rate at the upstream end of the channel. The water discharge Q_w and the sediment discharge Q_s are varied independently in the range $0.6 - 2.4$ L/min and $0.07 - 4.4$ g/min, respectively. The sediment discharge is imposed by an industrial volumetric feeder using a spiral helix (Gericke).

At the outlet, the sediment layer is held by a 3 cm slat over which water and sediments run to exit the channel. Assuming that sediment transport is homogeneous across the channel, the local particle flux reads

$$q_x = \frac{Q_s}{W},\tag{2}$$

where Q_s is expressed in grains per second (s^{-1}). After about one day, the experiment reaches a steady state (the bed elevation does not evolve any more).

As the flow-induced shear stress increases, more grains are entrained and the sediment discharge increases (figure 2). In most experimental set-ups, the shear stress is imposed and the sediment flux varies accordingly[16]. Here we impose the sediment discharge and measure the shear stress, once the experiment has reached its steady state. This method allows us to sustain long experiments without recirculating the sediments[15].

The flow is only a few millimeters deep, thus maintaining the Reynolds number Re $= Q_w/(W\nu)$ between 500 and 1400 (where ν is the viscosity of water). The flow aspect ratio remains larger than 10. The particle Reynolds number Re$_s = u\,d_s/\nu$ is about 25 (u is the flow velocity at the grain scale). Injecting dye in the channel indicates that the flow is laminar.
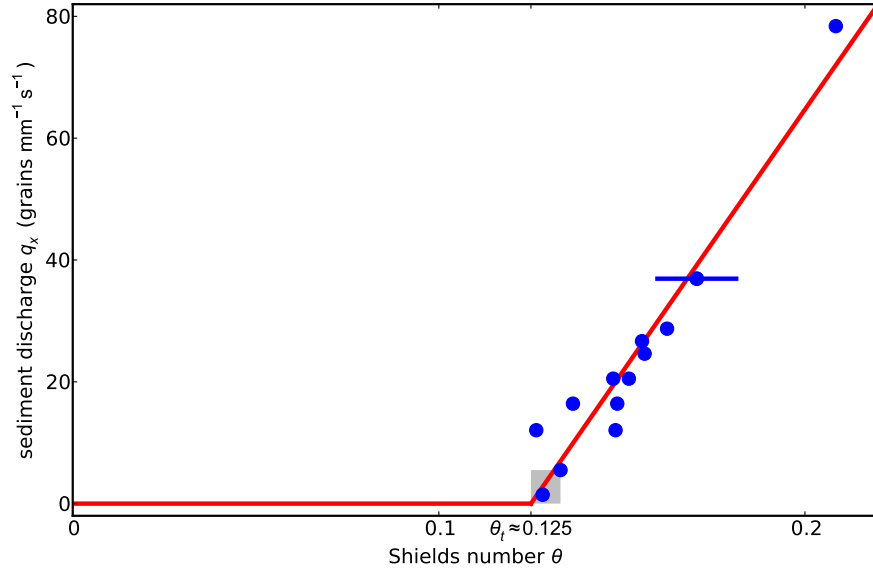
FIG. 2. Imposed bedload flux q_x as a function of the measured Shields parameter θ (blue dots). The transport law (14) is fitted to the data (red line, $q_x = \alpha V_s \, \theta_t \, (\theta - \theta_t)/d_s^2$ with $\alpha = 0.025$ and $\theta_t = 0.125$). The particle tracking experiments are limited to the shaded area.

Assuming a Hagen-Poiseuille velocity profile, the shear stress τ reads[31,32]

$$\tau = \rho \; (S \, g)^{2/3} \left(\frac{3 \, Q_w \, \nu}{W} \right)^{1/3} \tag{3}$$

where ρ, S and g are the density of water, the bed slope, and the gravity acceleration respectively.

The slope varies between $S = 0.008$ and $S = 0.0016$. It is measured with respect to a plumb line on pictures with a $0.3\,\text{mm/pixel}$ resolution. Using equation(3), we evaluate the shear stress with an accuracy of about 10 %.

B. Erosion and deposition

If the flow-induced stress is strong enough to overcome the weight of a bed particle, the latter gets entrained as bedload. This is usually expressed in terms of the Shields parameter θ, that is, the ratio of the shear stress to the weight of a grain[5]:

$$\theta = \frac{\tau}{(\rho_s - \rho) \, g \, d_s} \, . \tag{4}$$

Bedload transport starts when the Shields parameter crosses the threshold θ_t, and further increases with shear stress (figure 2). According to equation (1), this increase results either from faster particles, from a more concentrated bedload layer, or from any combination of the two.

To identify what primarily controls bedload near the threshold of motion, we now re-interpret the erosion-deposition model in the neighborhood of the critical Shields parameter.

Let us first consider the entrainment of a particle initially at rest. The flow applies a viscous drag f_ν on the particle, while the bed friction opposes the drag. When the particle gets entrained, the viscous drag is proportional to the fluid velocity u with respect to the particle velocity V_e:

$$f_\nu \sim \rho \, \nu \, d_s^2 \, (u - V_e). \tag{5}$$

About a grain diameter above the bed surface, the fluid velocity is proportional to the shear rate, and consequently to the shear stress:

$$u \sim d_s \, \frac{\partial u}{\partial z} \; \sim \; d_s \, \frac{\tau}{\rho \nu} \sim V_s \, \theta \tag{6}$$

where z is the vertical coordinate and $V_s = (\rho_s - \rho)\,g\,d_s^2/(18\,\rho\,\nu)$ is Stokes's settling velocity (for our particles, $V_s \approx 3.3\,\mathrm{cm\,s^{-1}}$). Here, this velocity appears only as a scale (as opposed to a vertical velocity).

When the viscous drag overcomes the Coulomb friction on the bed, the bed particle gets entrained. If the grain Reynolds number is low enough, we can neglect the particle inertia during the entrainment process. The viscous drag then balances Coulomb's friction, which scales like the particle weight:

$$f_\nu \sim (\rho_s - \rho)\,g\,d_s^3 \tag{7}$$

Combined with relations (5) and (6), the above balance reads

$$V_e \sim V_s\,(\theta - \theta_t) \tag{8}$$

where θ_t is, at this point, an arbitrary dimensionless coefficient. Naturally, we identify it with the threshold Shields parameter since the grain velocity vanishes when $\theta = \theta_t$. The above expression results from the balance between viscous drag and gravity. It is therefore valid only as long as the particle remains in contact with immobile particles, that is, during the entrainment process.

A bed particle belongs to the bedload layer when it has escaped its neighbors, which takes a characteristic time of about d_s/V_e. We expect the average entrainment rate to be proportional to the inverse of this time, and to the bed surface concentration $1/d_s^2$:

$$\dot{n}_e \sim \frac{V_s}{d_s^3}\,(\theta - \theta_t)\,. \tag{9}$$

Once it has joined the bedload layer, a particle travels, on average, at the velocity of the fluid. Thus, after equation (6),

$$V_x \sim V_s\,\theta\,. \tag{10}$$

At order zero in $\theta - \theta_t$, the velocity of bedload particles is therefore independent of the Shields stress:

$$V_x \sim V_s\,\theta_t. \tag{11}$$

As it travels downstream, a bedload particle bounces on the bed surface at a characteristic frequency V_x/d_s. Each time the particle hits the bed, it has a chance to get trapped. If the trapping probability is uniform, the deposition rate is proportional to the density of moving particles times the bouncing frequency:

$$\dot{n}_s \sim \frac{n\,V_s}{d_s}\,. \tag{12}$$

In steady state, the settling and erosion rate compensate each other ($\dot{n}_e = \dot{n}_s$). Thus, according to equations (12) and (9), we find that the concentration of moving grains is proportional to the shear stress in excess of the threshold:

$$n \sim \frac{\theta - \theta_t}{d_s^2}\,. \tag{13}$$

Finally, after equation (1), the sediment transport rate at steady state reads

$$q_x = \frac{\alpha\,V_s\,\theta_t}{d_s^2}\,(\theta - \theta_t)\,, \tag{14}$$

where α is a dimensionless parameter. This approximation proves valid over a broad range of shear stress (figure 2). The linear extrapolation of our data yields a threshold Shields stress of about 0.12, consistent with previous reports at similar particle Reynolds number[5,15,33].

The above reasoning illustrates the nature of bedload transport near the threshold: the properties of the moving particles are virtually independent of the shear stress (their average velocity is constant). The bedload layer is thus a collection of similar particles, and sediment transport
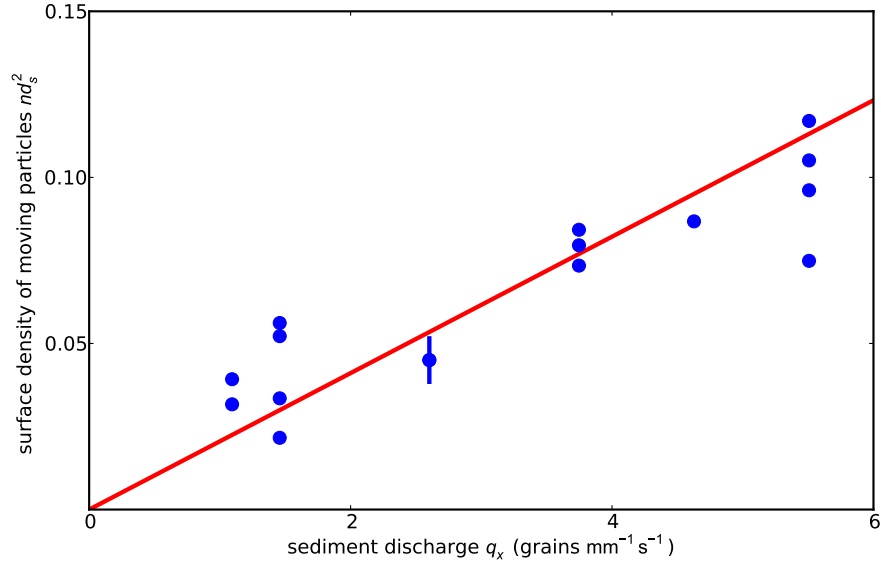
FIG. 3. Surface concentration of moving particles $n\,d_s^2$ as a function of the sediment discharge q_x. This data set corresponds to the shaded area of figure 2.

is the sum of individual particle movements. Consequently, the sediment flux increases in proportion to the concentration of moving grains, as long as the latter remains small ($n\,d_s^2 \ll 1$). Our experiments support this interpretation (figure 3).

Measuring accurately the bottom shear stress in a channel is challenging. To the contrary, computerized image processing allows us to count moving particles accurately. Moreover, the concentration of moving particles varies by a factor of about four in our experiments, while the Shields parameter varies by less than 10% (shaded area on figure 2). Finally, the flow is not perfectly uniform across the channel, due to surface tension and viscous friction on the walls, and the average Shields parameter might not represent adequately the local flow conditions. Accordingly, we choose to characterize the state of our system by the concentration of moving grains n, as measured by image processing. To vary this parameter, we change the sediment input. The channel slope then adjusts to the sediment discharge.

III. PARTICLE MOTION

A. Velocity

We record the motion of bedload particles with a camera placed above the water surface (100 frames per second, 1024×256 pixels). To isolate individual particles, we dye about 0.5% of the grains. The proportion of dyed particles is low enough to unambiguously identify a single particle on successive pictures of the experiment, and thus to follow its trajectory (figure 4). The center of mass of a particle is located with a precision of 50 μm on each picture (the particle diameter corresponds to about 10 pixels).

A particle moves essentially downstream, with an intermittent pace. It alternates between motion and rest, the succession of which is randomly distributed[15,16,25,34–36] (figure 4). When moving, a particle rolls, slides and sometimes gets lifted a few grain diameters above the bed surface.

Although the velocity of moving particles varies significantly, we can unambiguously distinguish between the bedload layer and the immobile bed surface on successive pictures. More specifically, we label a particle as "moving" if the standard deviation of its position over four successive pictures is larger than $0.1\,d_s$. This procedure allows us to separate actual motion from the flickering caused by small surface waves.

For each experimental run, we record about 10 independent movies, each of them containing
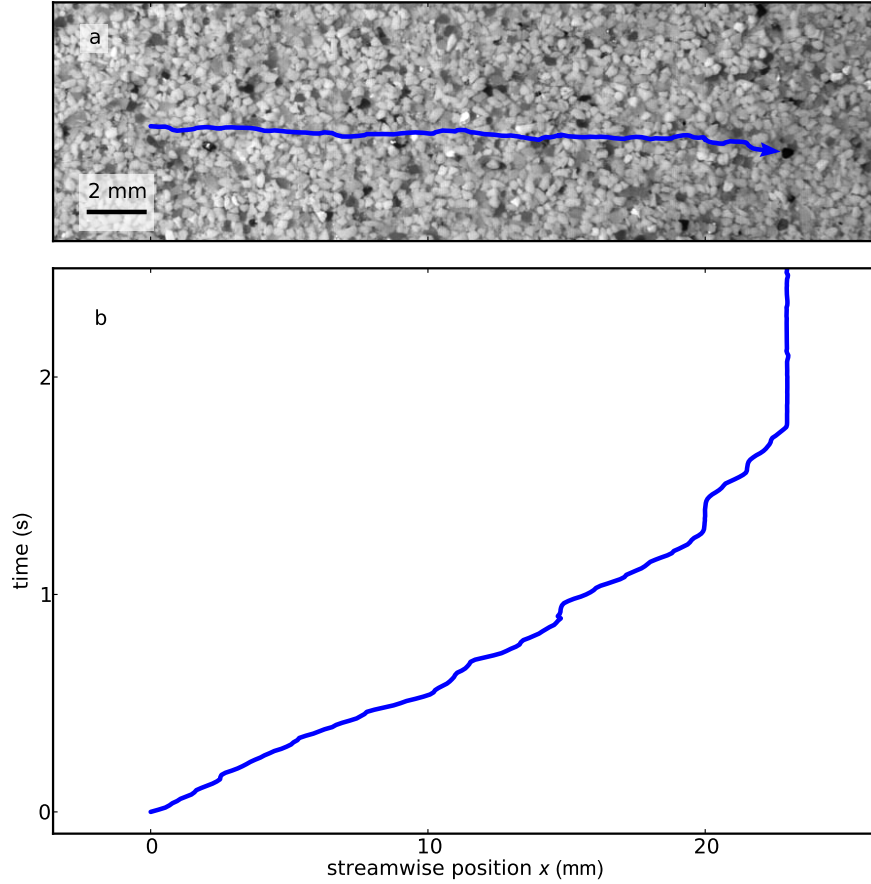
FIG. 4. (a) Particle trajectory seen through the water surface. (b) Streamwise position of the same particle x/d_s as a function of time. The final period of rest lasts more than two seconds, but was truncated for readability.

about $5\,000$ frames. After separating moving particles from immobile ones, we obtain between $5\,000$ and $10\,000$ particle trajectories for each run. Since a particle flight typically lasts much longer than the time between successive frames, we can measure the velocity distribution of moving particles (figure 5). The particle streamwise velocity appears to be of the order of the settling velocity V_s, and essentially positive, in accordance with equation (11).

We suspect that most negative values of the velocities are due to image processing errors. Indeed, when an unmarked particle flows above an immobile marked particle, the latter appears to move backwards. Such events represent less than 5 % of our data. We therefore believe that they do not affect significantly our results.

Discarding the negative velocities, an exponential function approximates reasonably the distribution f_x of streamwise velocity v_x, in accordance with previous experiments involving glass beads[15] or sand[16,25]:

$$f_x(v_x) = \frac{1}{V_x}\, e^{-v_x/V_x} \qquad (15)$$

where V_x is the average particle velocity introduced in the mass balance equation (1). Close to the threshold for sediment transport, we find that the average particle velocity does not depend on the particle concentration (figure 6), with an average over all experiments of

$$V_x/V_s = 0.38 \pm 0.03\,. \qquad (16)$$

This value compares favorably with equation (11) and with prior findings[15]. Hereafter, we only assume that the average particle velocity is well-defined and independent of n, without specifying the shape of the distribution.
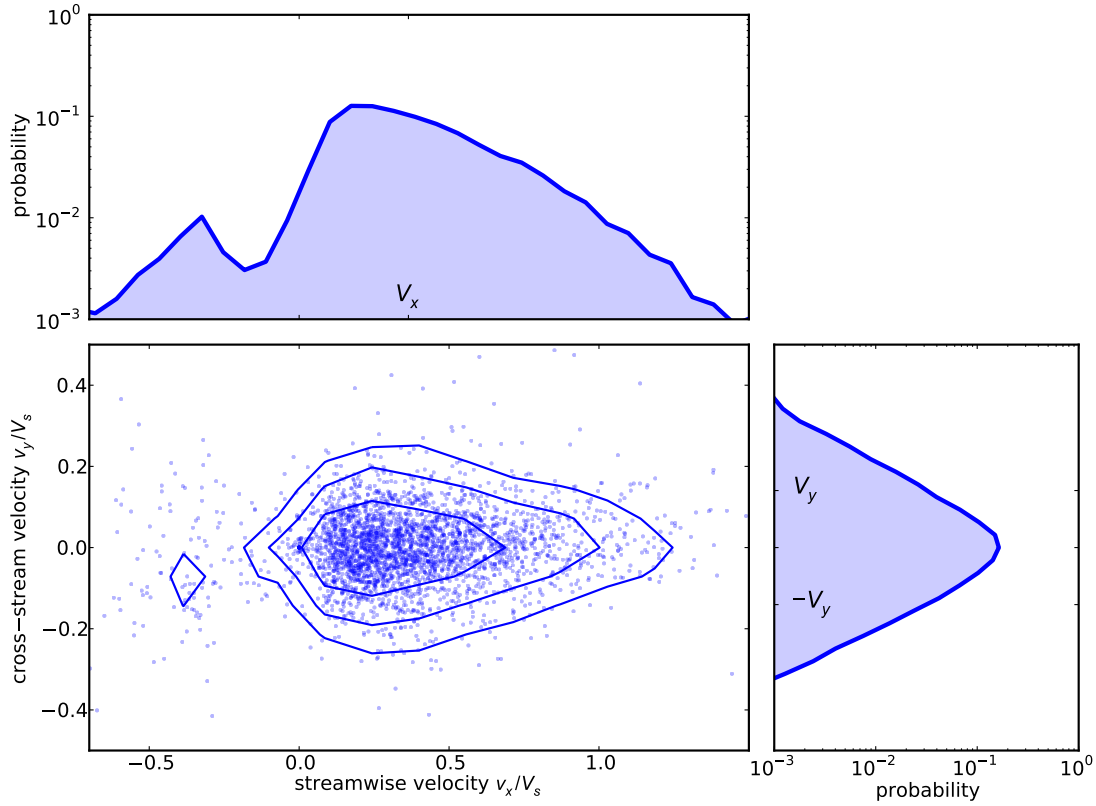
FIG. 5. Velocity distribution of moving particles, computed from about 15 000 individual velocities ($Q_w = 2.05$ L/min and $Q_s = 0.06$ g/min). The ticks indicate the average streamwise velocity and the cross-stream velocity variance.

As bedload particles move downstream, their cross-stream velocity v_y fluctuates around zero (figure 5). The distribution of cross-stream velocities is symmetrical, with typical velocities three times smaller than the streamwise velocity. The distribution, broader than a Gaussian, resembles a symmetric exponential function,

$$f_y(v_y) = \frac{1}{V_y} e^{-2|v_y|/V_y} \tag{17}$$

where V_y is the standard deviation of the cross-stream velocity. Again, this distribution is consistent with previous experimental findings[25]. Like the streamwise velocity, the cross-stream velocity does not depend on the concentration of moving particles (figure 6), and we find a standard deviation of $V_y/V_s = 0.12 \pm 0.02$ (average over all experiments).

B. Cross-stream spreading

As the grains are entrained by the flow, they also disperse stochastically in the cross-stream direction (figure 7). On average, bedload particles do not move across the stream, but individual trajectories drift away from the x axis due to fluctuations of the cross-stream velocity.

To quantify the spreading of bedload particles, we track the trajectories of a large number of them ($N \approx 7\,500$), and compute the variance σ_y^2 of their position across the channel:

$$\sigma_y^2(x) = \frac{1}{N} \sum_{i=1}^{N} y_i(x)^2 \tag{18}$$

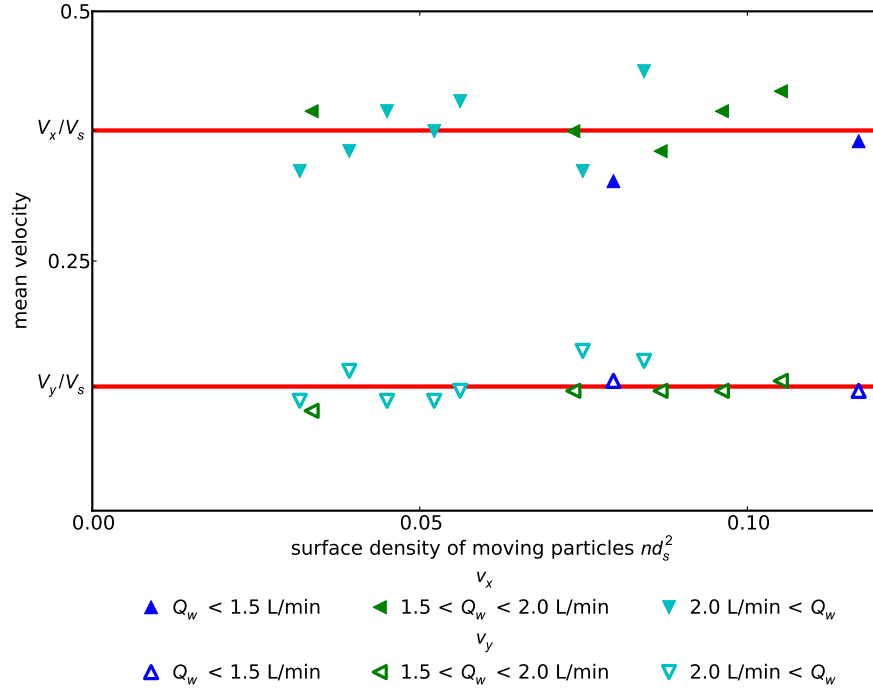where $y_i(x)$ is the trajectory of the i-th particle in the horizontal plane. The trajectories are

FIG. 6. Mean streamwise velocity (V_x/V_s, filled triangles) and cross-stream velocity variance (V_y/V_s, empty triangles) as a function of the number of moving particles, $n\,d_s^2$. Symbols and colors changes with water discharge.

shifted so that they all start from zero ($y_i(0) = 0$). The variance σ_y^2 represents the average spreading of a particle as a function of downstream distance, regardless of travel time.

We find that the variance increases linearly with the downstream distance (figure 7), which defines a diffusion length ℓ_d such that

$$\sigma_y^2 = 2\,\ell_d\,x\,. \tag{19}$$

For instance, $\ell_d = 9.5 \pm 0.8\,\mu\text{m}$ in figure 7, that is, about $0.028\,d_s$. Repeating the same procedure for all experimental runs, we observe that the diffusion length ℓ_d is independent of the concentration of moving particles, within the range explored here (figure 8). On average over all experiments, we find a diffusion length of

$$\frac{\ell_d}{d_s} = 0.030 \pm 0.004. \tag{20}$$

This value is about ten times smaller than the diffusion length of a ball rolling down a slope covered with fixed grains[37]. In our experiment, the fluid probably attenuates the bed influence on moving particles.

C. Random walk

The linear dependence of the particle dispersion with respect to the travel distance evokes a random walk. To elaborate on this analogy, let us represent the bedload particle as a walker which takes a random step of length δ_y in the cross-stream direction each times it travels downstream over a distance δ_x. A more physical picture, perhaps, is to consider that a moving particle deflects off immobile particles as it travels downstream. Accordingly, we expect both δ_x and δ_y to scale with the grain diameter.

The walker's trajectory is a sum of successive steps, the variance of which reads

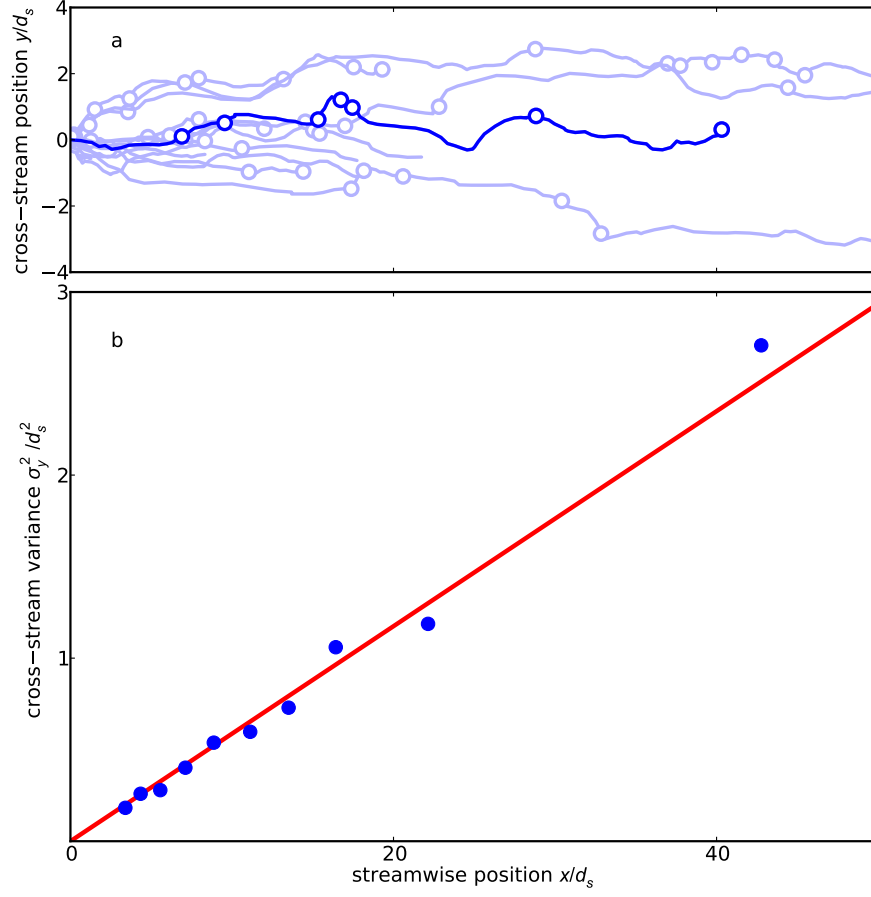$$\sigma_y^2 = \frac{\delta_y^2}{\delta_x}x \tag{21}$$

FIG. 7. (a) Particle trajectories in the horizontal plane (same experimental run as Figure 5). The trajectories have been translated to collapse their origin. Empty dots indicate rest. The aspect ratio is exaggerated in the cross-stream direction. (b) Cross-stream variance of the particle position σ_y^2 as a function of the streamwise position x ($Q_w = 2.05$ L/min and $Q_s = 0.06$ g/min).

where x is the downstream distance from the starting point. We can identify the above relation with equation (19), which provides an interpretation for the diffusion length:

$$\ell_d = \frac{\delta_y^2}{2\,\delta_x}. \tag{22}$$

The random walk analogy is meaningful only if we can define an average step length (that is, a decorrelation length). Since the particle velocity has well-defined averages in both directions (section III A), we simply need to ascertain the existence of a decorrelation time. To do so, we compute the autocorrelation function of the cross-stream velocity. Averaging over a large number of trajectories, we find that the autocorrelation decays exponentially with time (figure 9). This decay defines a decorrelation time t_c, which can be averaged over all experimental runs:

$$\frac{t_c\,V_s}{d_s} = 1.0 \pm 0.1\,. \tag{23}$$

After equation 16, we find $t_c \approx 0.38\,d_s/V_x$, which is about the time to pass an immobile grain at velocity V_x. Equivalently, the decorrelation distance $t_c\,V_x$ compares with d_s, and consequently compares to the bed roughness.

To be consistent with the random walk analogy, we expect the downstream and cross-stream step lengths to satisfy

$$\delta_x \approx V_x\,t_c\,, \quad \delta_y \approx V_y\,t_c\,. \tag{24}$$
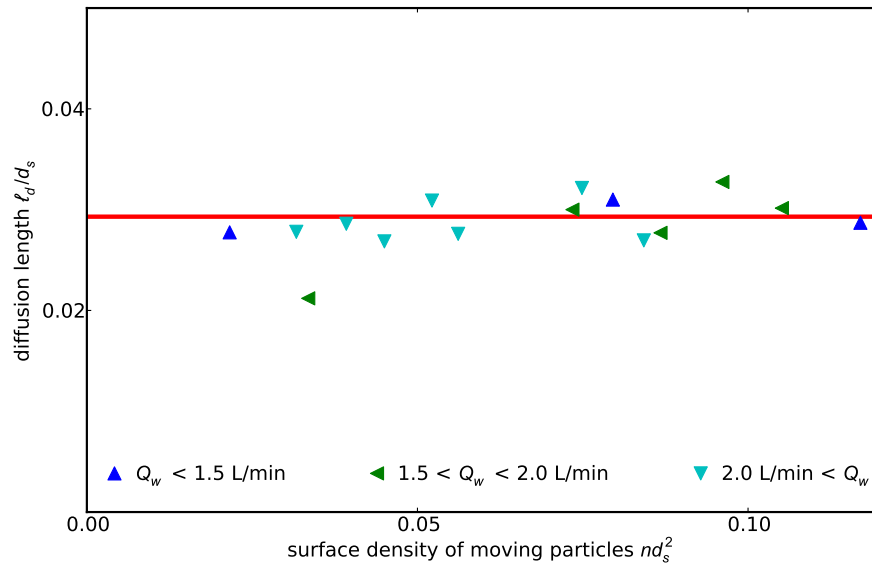
FIG. 8. Dependence of the diffusion length ℓ_d/d_s on the concentration of moving particles $n\,d_s^2$. The red line indicates the mean diffusion length.

Accordingly, using equation (22), we obtain an independent measurement of the diffusion length:

$$\ell_d = \frac{V_y^2\,t_c}{2\,V_x}\;.\tag{25}$$

Replacing the average velocities with their experimental values, we find $\ell_d/d_s = 0.02 \pm 0.01$, in reasonable accord with equation (20).

The step length of the random walk is about the size of a particle: $\delta_x \approx 0.4\,d_s$, which is much shorter than a typical particle flight (figure 4). Thus, the velocity decorrelation that causes dispersion occurs many times before the particle settles down, probably due to the roughness of the bed surface.

IV. DISCUSSION AND CONCLUSION

The experiments presented here, based on particle tracking, supports the erosion-deposition model of bedload transport, at least near the threshold Shields parameter. In addition we observe that, at first order, the statistical properties of the moving particles do not depend on their concentration n. We thus propose the following interpretation of bedload transport near threshold.

The moving particles constitute a thin layer travelling downstream at constant velocity. In steady state, this layer exchanges particles with the underlying sediment bed while maintaining its concentration n. As a result of the bed roughness, or of the associated flow perturbation, bedload particles disperse sideways as they progress downstream, like a ball rolling down a bumpy surface.

An inevitable attribute of any collection of random walkers is diffusion. Therefore, a cross-stream gradient of the bedload particles density induces a Fickian flux of particles towards the less populated areas. As long as the particles do not interact with each other, the diffusion flux is proportional to the concentration gradient:

$$q_y = -D\,\frac{\partial n}{\partial y}\tag{26}$$

where D is the diffusion coefficient associated to bedload transport. Based on our experiments,
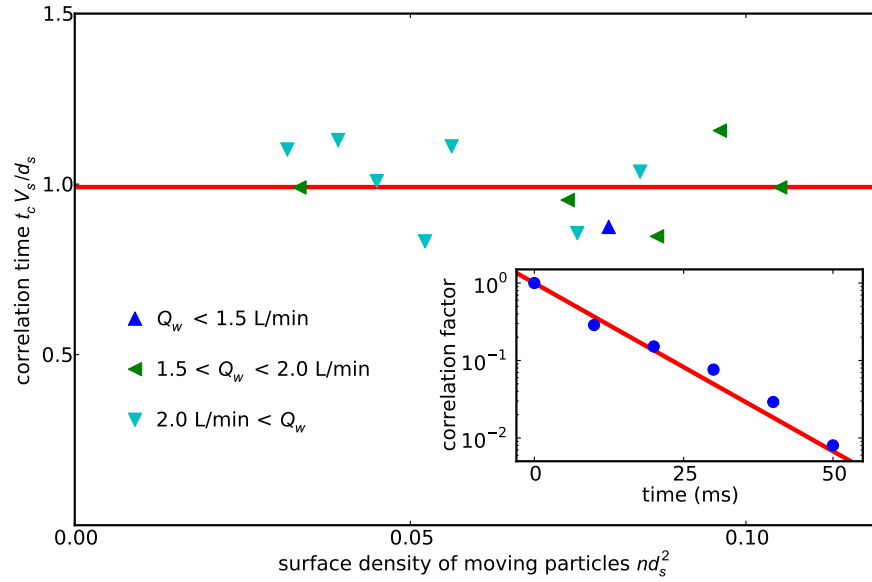
FIG. 9. Mean correlation time $t_c\, V_s/d_s$ as a function of the concentration of moving particles $n\, d_s^2$. The red dashed line shows the average correlation time. Inset: correlation between successive images as function of time (same run as Figure 5). The red line shows a fitted exponential decay.

we expect it to read

$$D = \ell_d\, V_x = \frac{V_y^2\, t_c}{2} \approx 0.03\, V_s\, d_s\,. \tag{27}$$

Since the streamwise flux of sediment q_x is the product of the particles velocity with their concentration, an equivalent expression of the diffusive flux is

$$q_y = -\ell_d\, \frac{\partial q_x}{\partial y}\,, \tag{28}$$

which might prove more practical than equation (27).

To measure directly this diffusive flux, one needs to produce a cross-stream gradient of bedload transport. For instance, a ring channel could generate a stronger shear near the outer wall[15], and thus induce a concentration gradient. If the findings of the present paper are confirmed, cross-stream diffusion will very likely be found in natural systems, where cross-stream gradients of bedload are ubiquitous.

The continual exchange of particles between the beload layer and the immobile bed plays no role in the above reasoning since, on average, a new particle is entrained for each deposited particle. The fate of individual particles, on the contrary, depends crucially on this transfer. The longer a particle remains part of the bedload layer, the faster it travels downstream. The random nature of erosion and deposition thus disperse the bedload particles along the flow direction. This is the subject of present research[38].

[1] W. Dietrich and J. Smith, "Bed load transport in a river meander," Water Resources Research **20** (1984).

[2] B. Gomez, "Bedload transport," Earth-Science Reviews **31**, 89–132 (1991).

[3] W. Graf and M. Altinakar, *Hydraulique Fluviale, Ecoulement non permanent et phenomenes de transport* (Eyrolles, Paris, 1996).

[4]M. Yalin and A. da Silva, *Fluvial Processes* (IAHR, 2001).

[5]A. S. Shields, "Anwendung der aehnlichkeitsmechanik und der turbulenzforschung auf die geschiebebewegung," Mitt. Preuss. Vers. Wasser. Schiff. **26** (1936).

[6]E. Meyer-Peter and R. Müller, "Formulas for bed-load transport," in *Proceedings of the 2nd Meeting of the International Association of Hydraulic Research*, Stockholm, Sweden (International Association of Hydraulic Research, 1948) pp. 39–64.

[7]H. Einstein, "The bed-load function for sediment transportation in open channel flows," Tech. Rep. 1026 (US Dept. of Agriculture, 1950).

[8]K. Ashida and M. Michiue, "Studies on bed-load transport rate in open channel flows," in *IAHR Int. Symp. River Mech., Bangkok, 1* (1973) pp. 407–417.

[9]R. Fernandez-Luque and R. Van Beek, "Erosion and transport of bed-load sediment," Journal of Hydraulic Research **14**, 127–144 (1976).

[10]F. Engelund and J. Fredsoe, "A sediment transpot model for straight alluvial channels," Nordic Hydrol. **7**, 293–306 (1976).

[11]J. Bridge and D. Dominic, "Bed load grain velocity and sediment transport rates," Water Resources Research **20**, 476–490 (1984).

[12]L. Van Rijn, "Sediment transport, part i: bed load transport," Journal of hydraulic Engineering **110**, 1431–1456 (1984).

[13]Y. Nino and M. Garcia, "Gravel saltation. part i: Experiments," Water Resources Research **30**, 1907–1914 (1994).

[14]C. Ancey, A. Davison, T. Bohm, M. Jodeau, and P. Frey, "Entrainment and motion of coarse particles in a shallow water stream down a steep slope," J. Fluid Mech. **595**, 83–114, doi: 10.1017/S0022112007008774 (2008).

[15]F. Charru, H. Mouilleron, and O. Eiff, "Erosion and deposition of particles on a bed sheared by a viscous flow," Journal of Fluid Mech. **519**, 55–80 (2004).

[16]E. Lajeunesse, L. Malverti, and F. Charru, "Bedload transport in turbulent flow at the grain scale: experiments and modeling," J. Geophys. Res. Earth Surface **115**, F04001, doi:10.1029/2009JF001628 (2010).

[17]F. Charru and E. Hinch, "Ripple formation on a particle bed sheared by a viscous liquid. part 1. steady flow," J. Fluid Mech. **550**, 111–121 (2006).

[18]F. Charru, "Selection of the ripple length on a granular bed sheared by a liquid flow," Phys. Fluids **18**, 121508–1–121508–9, doi: 0.1017/S002211200500786X (2006).

[19]O. Devauchelle, L. Malverti, E. Lajeunesse, P. Y. Lagrée, C. Josserand, and K. D. N. Thu-Lam, "Stability of bedforms in laminar flows with free surface: from bars to ripples," Journal of Fluid Mechanics **642**, 329–348 (2010).

[20]M. Houssais and E. Lajeunesse, "Bedload transport of a bimodal sediment bed," J. Geophys. Res **117**, F04015 (2012).

[21]C. Ancey, "Stochastic modeling in sediment dynamics: Exner equation for planar bed incipient bed load transport conditions," J. Geophys. Res **115**, F00A11, doi:10.1029/2009JF001260 (2010).

[22]O. Durán, B. Andreotti, and P. Claudin, "Numerical simulation of turbulent sediment transport, from bed load to saltation," Physics of fluids **24**, 103306 (2012).

[23]T. Revil-Baudard and J. Chauchat, "A two-phase model for sheet flow regime based on dense granular flow rheology," Journal of Geophysical Research: Oceans **118**, 619–634 (2013).

[24]D. Furbish, P. Haff, J. Roseberry, and M. Schmeeckle, "A probabilistic description of the bed load sediment flux: 1. theory," Journal of Geophysical Research **117**, F03031 (2012).

[25]J. Roseberry, M. Schmeeckle, and D. Furbish, "A probabilistic description of the bed load sediment flux: 2. particle activity and motions," Journal of Geophysical Research **117**, F03032 (2012).

[26]D. Furbish, J. Roseberry, and M. Schmeeckle, "A probabilistic description of the bed load sediment flux: 3. the particle velocity distribution and the diffusive flux," Journal of Geophysical Research **117**, F03033 (2012).

[27]D. Furbish, A. Ball, and M. Schmeeckle, "A probabilistic description of the bed load sediment flux: 4. fickian diffusion at low transport rates," Journal of Geophysical Research **117**, F03034 (2012).

[28]G. Parker, "Self-formed straight rivers with equilibrium banks and mobile bed. part 1. the sand-silt river," J. Fluid Mech. **89**, 109–125 (1978).

[29]O. Devauchelle, A. P. Petroff, A. E. Lobkovsky, and D. H. Rothman, "Longitudinal profile of channels cut by springs," Journal of Fluid Mechanics **667**, 38–47.

[30]G. Seizilles, O. Devauchelle, E. Lajeunesse, and F. Métivier, "Width of laminar laboratory rivers," Physical Review E **87**, 052204 (2013).

[31]L. Malverti, E. Lajeunesse, and F. Métivier, "Small is beautiful: upscaling from microscale laminar to natural turbulent rivers," Journal of Geophysical Research **113**, F04004 (2008).

[32]E. Lajeunesse, L. Malverti, P. Lancien, L. Armstrong, F. Metivier, S. Coleman, C. Smith, T. Davies, A. Cantelli, and G. Parker, "Fluvial and submarine morphodynamics of laminar and near-laminar flows: a synthesis," Sedimentology **57**, 1–26 (2010).

[33]J. Agudo and A. Wierschem, "Incipient motion of a single particle on regular substrates in laminar shear flow," Physics of Fluids **24**, 093302 (2012).

[34]F. Charru, E. Larrieu, J.-B. Dupont, and R. Zenit, "Motion of a particle near a rough wall in a viscous shear flow," J. Fluid Mech. **570**, 431–453 (2007).

[35]A. Lobkovsky, A. Orpe, R. Molloy, A. Kudrolli, and D. Rothman, "Erosion of a granular bed driven by laminar fluid flow," Journal of Fluid Mechanics **605**, 47–58 (2008).

[36]R. Martin, D. Jerolmack, and R. Schumer, "The physical basis for anomalous diffusion in bed load transport," Journal of Geophysical Research **117**, F01018 (2012).

[37]L. Samson, I. Ippolito, G. Batrouni, and J. Lemaitre, "Diffusive properties of motion on a bumpy plane," The European Physical Journal B-Condensed Matter and Complex Systems **3**, 377–385 (1998).

[38] E. Lajeunesse, O. Devauchelle, M. Houssais, and G. Seizilles, "Advection and exchange in bedload transport," Advances in Geosciences - in press.